Chapter 11

Reinterpretation in the pMSSM

After having discussed to some extent efforts and methods to reinterpret ATLAS searches for SUSY, this chapter presents a reinterpretation of the 1ℓ search in the pMSSM. The truth analysis and simplified likelihoods discussed in chapters 9 and 10, respectively, are instrumental for the following sections.

11.1 Motivation

In today's searches for SUSY, it is common to use simplified models as a way of avoiding the necessity of having to deal with high-dimensional parameter spaces that are extremely challenging to sample and compare to data. The simplified model approach has also been used in the second part of this work, where results of the interpretation of the 1ℓ search in the $\tilde{\chi}_1^\pm\tilde{\chi}_2^0 \to Wh\tilde{\chi}_1^0\tilde{\chi}_1^0$ model have been presented. As has been discussed in sections 1.2.7 and 8.3, simplified models are however by no means complete SUSY models and only serve as proxies for more complex and realistic SUSY scenarios. As such, simplified model limits cannot trivially be translated into limits on model parameters of a more complete SUSY model and large-scale reinterpretations are necessary to understand the constraints today's SUSY searches set on realistic SUSY scenarios.

One class of more complete models, focussing on phenomenologically viable models, is the pMSSM, introduced in section 1.2.6. With its 19 parameters it offers much more complex SUSY scenarios while still being of somewhat manageable dimensionality. Still, large-scale reinterpretations in the pMSSM are computationally challenging and require a set of approximations as those introduced in chapters 9 and 10. In the following, the *simplified analysis* constructed using the smeared truth-level analysis and the simplified likelihood will be used as the sole method to evaluate a set of pMSSM models.

Although the following sections will be restricted to a reinterpretation of the 1ℓ search, efforts are ongoing in ATLAS to perform large-scale reinterpretations using a majority of the full Run 2 ATLAS searches for SUSY, most likely resulting in one of the most comprehensive set of ATLAS constraints on SUSY yet.

Table 11.1: Scan ranges used for each of the 19 pMSSM parameters. For parameters written with a modulus sign, both the positive and negative values are allowed. The term 'gen(s)' refers to generation(s). Flat priors are used to draw random values from within the given ranges.

Parameter	min	max	Note
$m_{\tilde{L}_1}$ $(= m_{\tilde{L}_2})$	10 TeV	10 TeV	Left-handed slepton (first two gens.) mass
$m_{\tilde{e}_1}$ $(= m_{\tilde{e}_2})$	10 TeV	10 TeV	Right-handed slepton (first two gens.) mass
$m_{\tilde{L}_3}$	10 TeV	10 TeV	Left-handed stau doublet mass
$m_{\tilde{e}_3}$	10 TeV	10 TeV	Right-handed stau mass
$m_{\tilde{Q}_1}$ $(= m_{\tilde{Q}_2})$	10 TeV	10 TeV	Left-handed squark (first two gens.) mass
$m_{\tilde{u}_1}$ $(= m_{\tilde{u}_2})$	10 TeV	10 TeV	Right-handed up-type squark (first two gens.) mass
$m_{\tilde{d}_1}$ $(= m_{\tilde{d}_2})$	10 TeV	10 TeV	Right-handed down-type squark (first two gens.) mass
$m_{\tilde{Q}_3}$	2 TeV	5 TeV	Left-handed squark (third gen.) mass
$m_{\tilde{u}_3}$	2 TeV	5 TeV	Right-handed top squark mass
$m_{\tilde{d}_3}$	2 TeV	5 TeV	Right-handed bottom squark mass
$\lvert M_1 \rvert$	0 TeV	2 TeV	Bino mass parameter
$\lvert M_2 \rvert$	0 TeV	2 TeV	Wino mass parameter
$\lvert \mu \rvert$	0 TeV	2 TeV	Bilinear Higgs mass parameter
M_3	1 TeV	5 TeV	Gluino mass parameter
$\lvert A_t \rvert$	0 TeV	8 TeV	Trilinear top coupling
$\lvert A_b \rvert$	0 TeV	2 TeV	Trilinear bottom coupling
$\lvert A_\tau \rvert$	0 TeV	2 TeV	Trilinear τ lepton coupling
M_A	0 TeV	5 TeV	Pseudoscalar Higgs boson mass
$\tan\beta$	1	60	Ratio of the Higgs vacuum expectation values

11.2 Model sampling and processing

11.2.1 Sampling

All signal models considered in the following are sampled from the pMSSM using the parameter ranges shown in table 11.1. Flat probability distributions are used to draw random values within the given ranges for each parameter and each unique set of pMSSM parameters generated that way is referred to as an independent pMSSM model.

As this work discusses a search for electroweakinos, the SUSY models drawn from the pMSSM are sampled with a special focus on the electroweak sector and said supersymmetric particles. This is achieved by setting the mass parameters of the first and second generation squarks as well as those of the sleptons to values much higher than those accessible at LHC energies, effectively decoupling them. For naturalness arguments, third generation squarks and the gluino are not strictly decoupled but set to sufficiently high values such as not to affect the electroweak sector too much. The lower and upper bounds on the 12 scanned parameters are chosen to yield a high density of models with electroweakino masses accessible at LHC energies without constraining the parameter space too much.

Once a value for each of the 19 pMSSM parameters has been chosen, a number of publicly available software packages are executed in order to compute the properties of each model point. In a first step, SPheno v4.0.5 [276, 277] is used to calculate the spectrum of the sparticles. The masses and branching fractions calculated with SPheno are used to determine the masses and

mixings of the Higgs sector using FeynHiggs v2.15.0 [278–280]. An additional SUSY spectrum calculation is performed in parallel with SoftSusy v4.1.8 [281]. Although the masses, mixings and branching fractions from SoftSusy will not directly be used in the following, the program is still required to complete successfully in order to reduce the number of pMSSM models with pathological properties. After the complete model spectrum has been calculated, the dark matter relic abundance of each model is determined with micrOMEGAs v5.0.8 [282, 283].

11.2.2 Selection and processing

In order to avoid models with pathological properties, all spectrum generators are required to complete execution without error. The cross section for surviving models is computed at NLO using Prospino v2.1 [284, 285]. Models with an inclusive cross section for all electroweak production processes below 0.07 fb are discarded as they would result in less than 10 expected signal events with an integrated luminosity of 139 fb^{-1}, not enough to be sensitive to with current electroweak SUSY searches. All models are further required to produce a lightest Higgs mass compatible with a range of ± 5 GeV of the SM Higgs mass experimentally measured[†].

No constraints on the computed cosmological LSP abundance are applied at this stage in order to give a more general view after the models are evaluated using the 1ℓ search. Experimental constraints from e.g. LEP are also not applied at this stage for the same reason.

Of the 10,000 unique models sampled from the pMSSM using the above prescription, 5152 models survive the constraints and requirements discussed in this section and are analysed using the simplified 1ℓ search. The majority of the models failing this selection step were rejected due to the cross section constraints.

11.2.3 Event generation

Event generation is performed using the software centrally provided by the ATLAS production system. The initial pair of sparticles with up to one additional parton in the ME are generated using the MadGraph5_aMC@NLO v2.6.1. [175, 176] generator. Next, Pythia8.230 [177] with the A14 tune is used for the hadronisation and PS, together with the NNPDF 2.3 LO [179] PDF set. The number of events N generated for each model is determined by

$$N = \sigma \times \mathcal{L}_{\text{eff}}, \tag{11.1}$$

where $\mathcal{L}_{\text{eff}} = 700\,\text{fb}^{-1}$ is an effective integrated luminosity and σ is the inclusive production cross section of the model. The number of events generated is capped at a minimum number of 10^4 and a maximum number of 10^6 truth-level events.

11.2.4 Truth-level analysis

All models passing event generation are evaluated using the smeared truth-level analysis described in section 9.4. This is the only evaluation done for the models considered in this

[†] The mass range is based on a conservative estimate of the theoretical uncertainties arising from the FeynHiggs calculation.

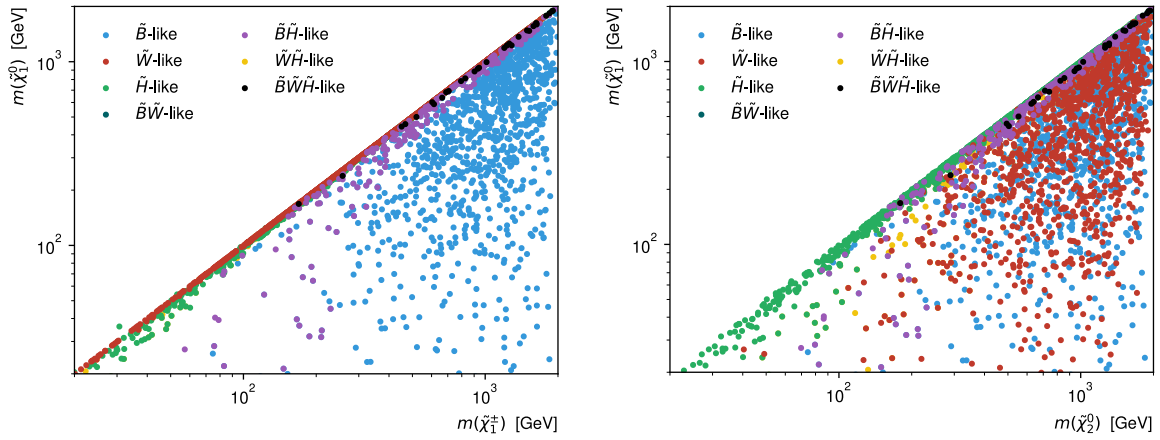

(a) **(b)**

Figure 11.1: Scatter plot of all models sampled in the (a) $m(\tilde{\chi}_1^\pm)$–$m(\tilde{\chi}_1^0)$ and (b) $m(\tilde{\chi}_2^0)$–$m(\tilde{\chi}_1^0)$ planes. The colour encodes the composition of the $\tilde{\chi}_1^0$ in each model. The $\tilde{\chi}_1^0$ is considered to be bino-like ($\tilde{B}$-like), wino-like ($\tilde{W}$-like) or higgsino-like ($\tilde{H}$-like) if the corresponding fraction from the neutralino mass mixing matrix is at least 80%. Additionally, the $\tilde{\chi}_1^0$ is considered to be of mixed nature if more than one component has a fraction of 20%. For example, a $\tilde{B}\tilde{W}$-like $\tilde{\chi}_1^0$ has more than 20% bino and wino components, but less than 20% higgsino component.

thesis. A full scan over the pMSSM including multiple ATLAS searches would additionally include a processing step reverting to the full analysis available through RECAST for model points where (non-)exclusion is uncertain based on truth-level analysis only.

11.3 Phenomenology of the LSP

The composition of the $\tilde{\chi}_1^0$ in each pMSSM model sampled is shown in the $m(\tilde{\chi}_1^\pm)$–$m(\tilde{\chi}_1^0)$ and $m(\tilde{\chi}_2^0)$–$m(\tilde{\chi}_1^0)$ planes in figs. 11.1(a) and 11.1(b), respectively. The $\tilde{\chi}_1^0$ is considered to be bino-like ($\tilde{B}$-like), wino-like ($\tilde{W}$-like) or higgsino-like ($\tilde{H}$-like) if the corresponding fraction from the neutralino mass mixing matrix is at least 80%. If more than one component has a fraction of more than 20%, then the $\tilde{\chi}_1^0$ is considered to be of mixed nature. The nature of the LSP as a function of the mass parameters M_1, M_2 and μ is shown as a reference in fig. C.4.

In the bulk of the $m(\tilde{\chi}_1^\pm)$–$m(\tilde{\chi}_1^0)$ plane, i.e. the parameter space targeted by the 1ℓ search using the simplified model, a large majority of the models produce a bino-like LSP with nearly mass-degenerate $\tilde{\chi}_1^\pm$ and $\tilde{\chi}_2^0$. These models correspond to cases where $M_1 \ll \mu$ and $M_1 < M_2$ and are thus similar to the canonical simplified model considered in the 1ℓ search. Some sensitivity can be expected towards these models using the 1ℓ search, provided that the branching fractions of the decays $\tilde{\chi}_1^\pm \to W^\pm\tilde{\chi}_1^0$ and especially $\tilde{\chi}_2^0 \to h\tilde{\chi}_1^0$ are large enough and produce on-shell bosons.

Towards the diagonal of $m(\tilde{\chi}_1^\pm)$–$m(\tilde{\chi}_1^0)$ plane, i.e. for models where the $\tilde{\chi}_1^\pm$ and $\tilde{\chi}_1^0$ are nearly mass-degenerate, the nature of the LSP shows a larger variation. In a large set of models where M_2 is not too heavy and $M_2 \ll M_1, \mu$, the LSP has a significant wino component and is nearly

mass-degenerate with the $\tilde{\chi}_1^\pm$, while the $\tilde{\chi}_2^0$ can be more massive. In models where the LSP has a large higgsino component, i.e. $\mu \ll M_1, M_2$, all three electroweakinos $\tilde{\chi}_1^\pm$, $\tilde{\chi}_2^0$ and $\tilde{\chi}_1^0$ are nearly mass-degenerate and result in very soft decay products, making these models inherently difficult to target.

11.4 Impact of the search on the pMSSM

The impact of the 1ℓ search on the pMSSM is discussed using one-dimensional and two-dimensional distributions in the following sections. A model is considered to be excluded if the observed CL_s value obtained from the simplified likelihood using the smeared truth-level inputs is below 0.05. Of the 5152 models evaluated, the 1ℓ search excludes a total of 98, or about 1.9%, of the models.

For the one-dimensional distributions shown in the following, the total number of models is compared against the number of models excluded by the 1ℓ search. An additional pad indicates the ratio between models excluded and total models sampled in each bin of the distribution. In the two-dimensional distributions, the numbers in the bins indicate the number of pMSSM models falling into each bin. In these distributions, the fraction of models excluded with the 1ℓ search is encoded using the z-axis, represented by a colour bar. Bins in which all models are excluded are coloured in black, while bins without any excluded models are left white. Where applicable, the exclusion contour obtained by the 1ℓ search using the simplified model is overlaid.

11.4.1 Impact on electroweakino masses

Figures 11.2 and 11.3 show the bin-by-bin fractions of models excluded by the 1ℓ search as two- and one-dimensional distributions, respectively. From the $\tilde{\chi}_1^\pm$–$\tilde{\chi}_1^0$ plane in fig. 11.2(a), it can be seen that the 1ℓ search is most sensitive to pMSSM models in mass ranges similar to those excluded in the context of the simplified model. Most of the models excluded have $\tilde{\chi}_1^\pm/\tilde{\chi}_2^0$ masses ranging from roughly 200 GeV to about 700 GeV and LSP ranging masses from 0 GeV to about 300 GeV. The proportion of excluded models peaks at $m(\tilde{\chi}_1^\pm, \tilde{\chi}_2^0) \approx 450$ GeV and light LSPs with $\tilde{\chi}_1^0 < 150$ GeV, as visible in fig. 11.3.

The models excluded by the 1ℓ search can roughly be classified in two categories: models lying within the simplified model exclusion contour and models with nearly mass-degenerate $\tilde{\chi}_1^\pm$ and $\tilde{\chi}_2^0$. As discussed in section 11.3, most models within the simplified model exclusion contour produce a bino-like LSP and result in nearly mass-degenerate $\tilde{\chi}_1^\pm$ and $\tilde{\chi}_2^0$. Figure C.5 illustrates this behaviour further. Expectedly, the 1ℓ search is thus most sensitive to $\tilde{\chi}_1^\pm\tilde{\chi}_2^0$ production with wino-like electroweakinos and a bino-like $\tilde{\chi}_1^0$, corresponding to models with a spectrum close to that of the canonical simplified model signature originally considered in the search.

The second category of models excluded comprises cases where the LSP is wino-like and nearly mass-degenerate with the $\tilde{\chi}_1^\pm$, corresponding to the diagonal in fig. 11.2(a). As the mass difference between the LSP and the $\tilde{\chi}_1^\pm$ is typically of the order of a few 100 MeV the $\tilde{\chi}_1^\pm$ becomes long-lived and primarily decays to a LSP and a low-momentum, charged pion. If the $\tilde{\chi}_1^\pm$ is produced with large momentum, it can live long enough to traverse multiple layers of the ATLAS detector before decaying, leading to a disappearing track signature. Searches targeting

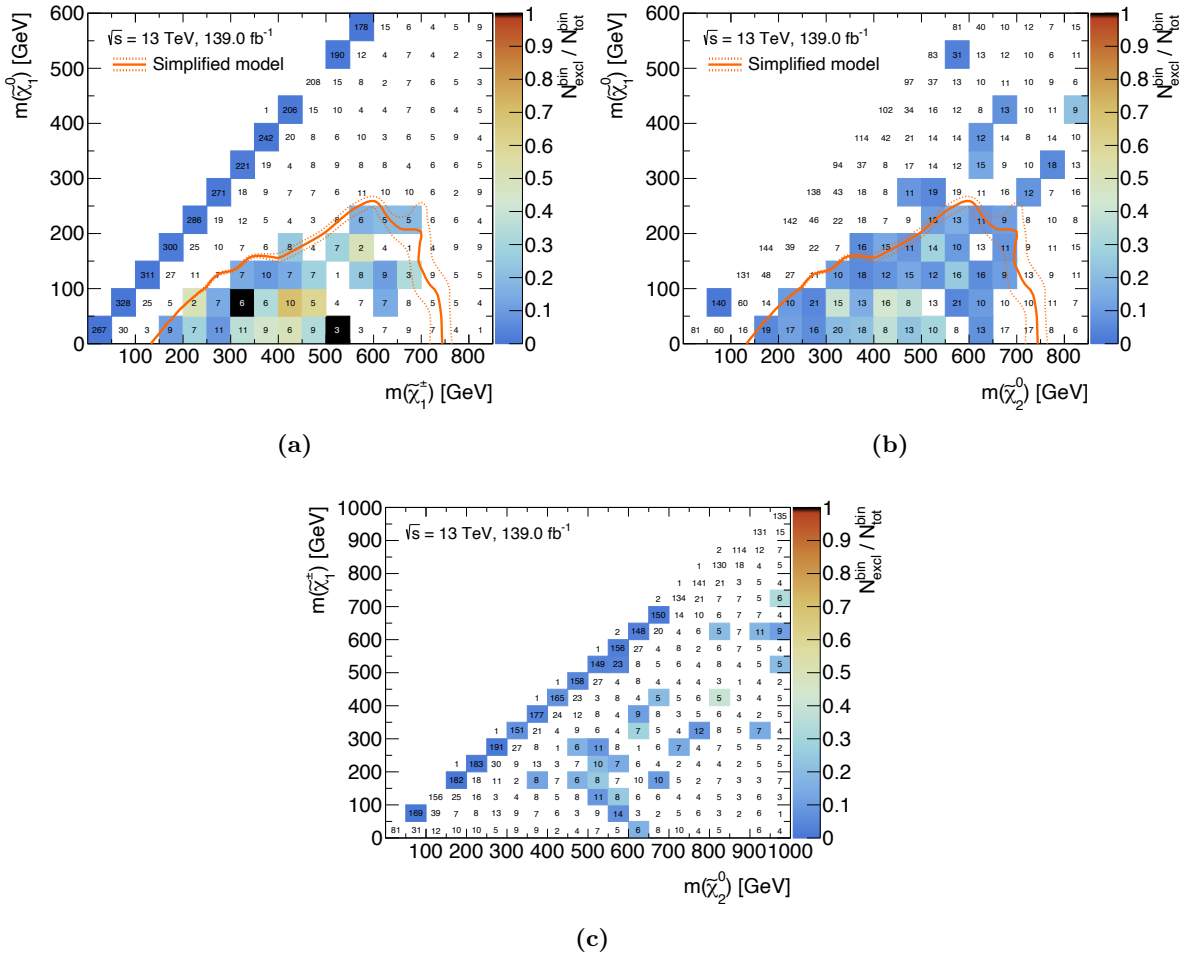

Figure 11.2: Bin-by-bin fraction of excluded models as a function of the relevant sparticle masses. The numbers in the bins correspond to the total number of models sampled falling into the respective bin. The number of models excluded by the 1ℓ search is encoded with a colour bar ranging from 0 to 1. Where all models in a given bin are excluded, the bin is coloured in black. Bins without any models excluded are left white. Models are evaluated using the simplified likelihood of the 1ℓ search. The simplified model contour is shown in orange.

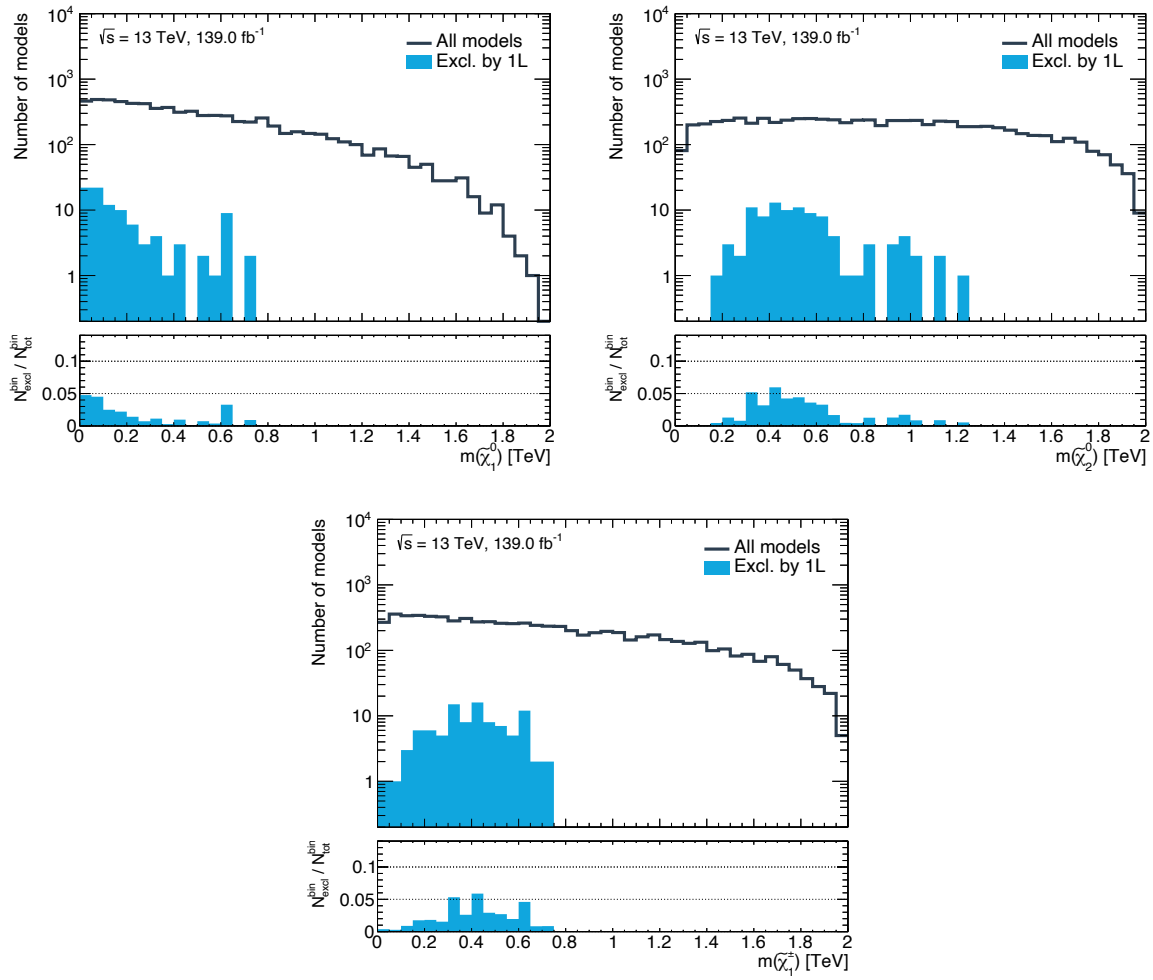

Figure 11.3: Bin-by-bin number of excluded models as a one-dimensional function of the electroweakino masses. The bin-wise fraction of excluded models, $N^{\text{bin}}_{\text{excl}}/N^{\text{bin}}_{\text{total}}$, is shown in the lower pad. All models are evaluated using the simplified likelihood of the 1ℓ search.

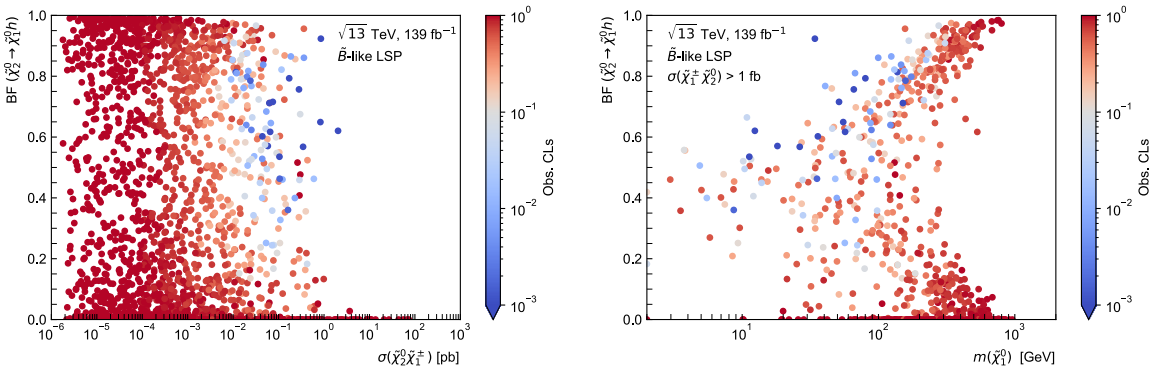

(a) **(b)**

Figure 11.4: Density of the pMSSM models with bino-like $\tilde{\chi}_1^0$ projected onto the plane spanned by (a) $\tilde{\chi}_1^\pm\tilde{\chi}_2^0$ pair-production cross section and BF($\tilde{\chi}_2^0 \to h\tilde{\chi}_1^0$) and (b) $m(\tilde{\chi}_1^0)$ and BF($\tilde{\chi}_2^0 \to h\tilde{\chi}_1^0$). The observed CL_s value obtained for each model using the 1ℓ search is encoded using the colour-palette. Models with a red tint cannot be excluded, models with a neutral white tint are on the boundary of exclusion, and models with a blue tint can be excluded. Only models satisfying $\sigma(\tilde{\chi}_1^\pm\tilde{\chi}_2^0) > 1\,\mathrm{fb}$ are shown in fig. (b).

prompt electroweakino decays are not expected to be sensitive to these models, and instead dedicated disappearing track searches are developed within ATLAS (cf. e.g. Ref. [286]). Even though no sensitivity to these models is expected from the 1ℓ search, a small set of models with a wino-like LSP can still be excluded. These models correspond to scenarios where the $\tilde{\chi}_2^\pm$ is not too heavy such that the 1ℓ search is sensitive to $\tilde{\chi}_2^\pm\tilde{\chi}_2^0$ production with cross sections of $\mathcal{O}(1\,\mathrm{fb})$. If the $\tilde{\chi}_2^\pm$ decays directly into the LSP via $\tilde{\chi}_2^\pm \to W^\pm\tilde{\chi}_1^0$, enough events with an isolated lepton can occur, allowing to exclude the model. (cf. fig. C.6(c)).

No sensitivity is observed for pMSSM models with higgsino-like electroweakinos and thus compressed mass spectra. This is expected, as the electroweakino decays in such scenarios typically produce off-shell W, Z and h bosons, resulting in very soft final state objects the 1ℓ search is not optimised for. Dedicated searches (see e.g. Ref. [272]) exist in ATLAS to target such compressed scenarios and work is ongoing to include these in the scans of the pMSSM.

In general, the sensitivity to pMSSM models is significantly reduced compared to the simplified model exclusion contour, even in the parameter space generating models with spectra similar to that of the simplified model. The crucial difference, responsible for the loss in sensitivity, is the fact that the simplified model assumes branching ratios of 100% of the $\tilde{\chi}_1^\pm \to W^\pm\tilde{\chi}_1^0$ and $\tilde{\chi}_2^0 \to h\tilde{\chi}_1^0$ decays (with on-shell W and h bosons). While the former is in general a good assumption in pMSSM models where $m(\tilde{\chi}_1^0) + m(W) \lesssim m(\tilde{\chi}_1^\pm) \lesssim m(\tilde{\chi}_2^0)$, the latter turns out not to be the dominant decay of the $\tilde{\chi}_2^0$ in many models where the decay $\tilde{\chi}_2^0 \to Z\tilde{\chi}_1^0$ dominates instead. The couplings of the $\tilde{\chi}_2^0$ to the Higgs boson are suppressed by powers of $|\mu|/M_2$ in the gaugino-like regions [287], meaning that the branching fraction of $\tilde{\chi}_2^0 \to h\tilde{\chi}_1^0$ takes on reasonably high values only in models with an LSP containing a substantial bino component. The Higgs coupling suppression is illustrated in fig. C.8. As can be seen from fig. 11.2(a), even in the bulk of the $\tilde{\chi}_1^\pm$–$\tilde{\chi}_1^0$ plane—containing mostly models with a bino-like LSP—not all models can be excluded by the simplified 1ℓ search. Figure 11.4 shows that many of these models have either a too small $\tilde{\chi}_1^\pm\tilde{\chi}_2^0$ pair-production cross section or too low values for BF($\tilde{\chi}_2^0 \to h\tilde{\chi}_1^0$). For the few non-excluded models with reasonable $\tilde{\chi}_1^\pm\tilde{\chi}_2^0$ pair-production cross

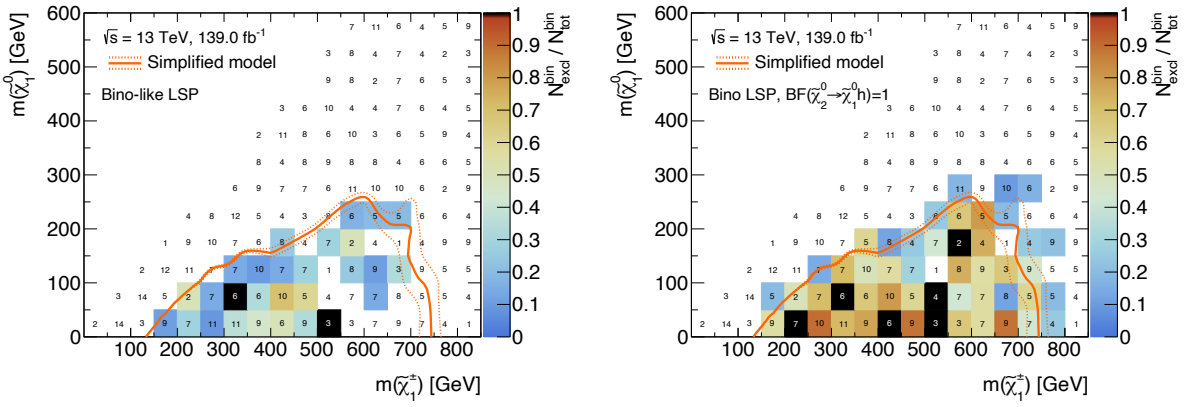

(a) Mixed BFs **(b)** $\mathrm{BF}(\tilde{\chi}_2^0 \to h\tilde{\chi}_1^0) = 1$

Figure 11.5: Bin-by-bin fraction of excluded models with a bino-like $\tilde{\chi}_1^0$ as a function of $m(\tilde{\chi}_1^\pm)$ and $m(\tilde{\chi}_1^0)$. In fig. (a) the pMSSM models originally sampled are shown. In fig (b), the $\mathrm{BF}(\tilde{\chi}_2^0 \to h\tilde{\chi}_1^0)$ is hard-coded to 100% after which event generation and 1ℓ analysis evaluation are re-exectued. Only models with a bino-like LSP are shown.

section $\sigma(\tilde{\chi}_1^\pm \tilde{\chi}_2^0) \gtrsim 1\,\mathrm{fb}$ and high enough Higgs coupling to $\tilde{\chi}_2^0$, the mass of the LSP turns out to be too high ($m(\tilde{\chi}_1^0) \gtrsim 250\,\mathrm{GeV}$), typically resulting in final states with insufficient $E_\mathrm{T}^\mathrm{miss}$ and soft objects.

As a cross-check, a significant portion of the models with bino-like LSP were reprocessed with $\mathrm{BF}(\tilde{\chi}_2^0 \to h\tilde{\chi}_1^0)$ fixed to unity (and $\mathrm{BF}(\tilde{\chi}_2^0 \to Z\tilde{\chi}_1^0)$ consequently set to disappear) and subsequently analysed with the 1ℓ search. Figure 11.5(b) reveals that significantly more models can be excluded within the simplified model contour when the simplified model branching fraction assumption is restored. As the $\tilde{\chi}_2^0$ decay into a Z boson and $\tilde{\chi}_1^0$ is the competing decay to $\tilde{\chi}_2^0 \to h\tilde{\chi}_1^0$, statistically combining searches targeting these decay modes could recover the loss in sensitivity. Likewise, the development of searches targeting both decay modes at the same time, would also recover the full sensitivity[†].

11.4.2 Impact on pMSSM parameters

The impact of the 1ℓ search on the pMSSM parameters relevant to the electroweak sector are shown in one-dimensional distributions in fig. 11.6. As already discussed in section 11.4.1, the 1ℓ search has the largest impact for small values in the bino mass parameter M_1, leading to models with a bino-like LSP when $M_1 \ll M_2, \mu$. Consequently, the proportion of excluded models peaks at slightly higher values in the distribution of the wino mass parameter, $|M_2| \approx 400\,\mathrm{GeV}$. As the search is not sensitive to compressed scenarios with a higgsino-like LSP, no models with small values in $|\mu|$ can be excluded.

As the pseudoscalar Higgs boson does not directly enter the phenomenology of the models targeted by the 1ℓ search, only indirect constraints are provided on m_A, excluding models in the full range of the m_A distribution sampled. A similar behaviour is observed in $\tan\beta$ where the excluded models have values of $\tan\beta$ spanning the full range from 1 to 60. Likewise, no

[†] Provided that they are targeted with disjoint signal regions such that a combined likelihood can be built.

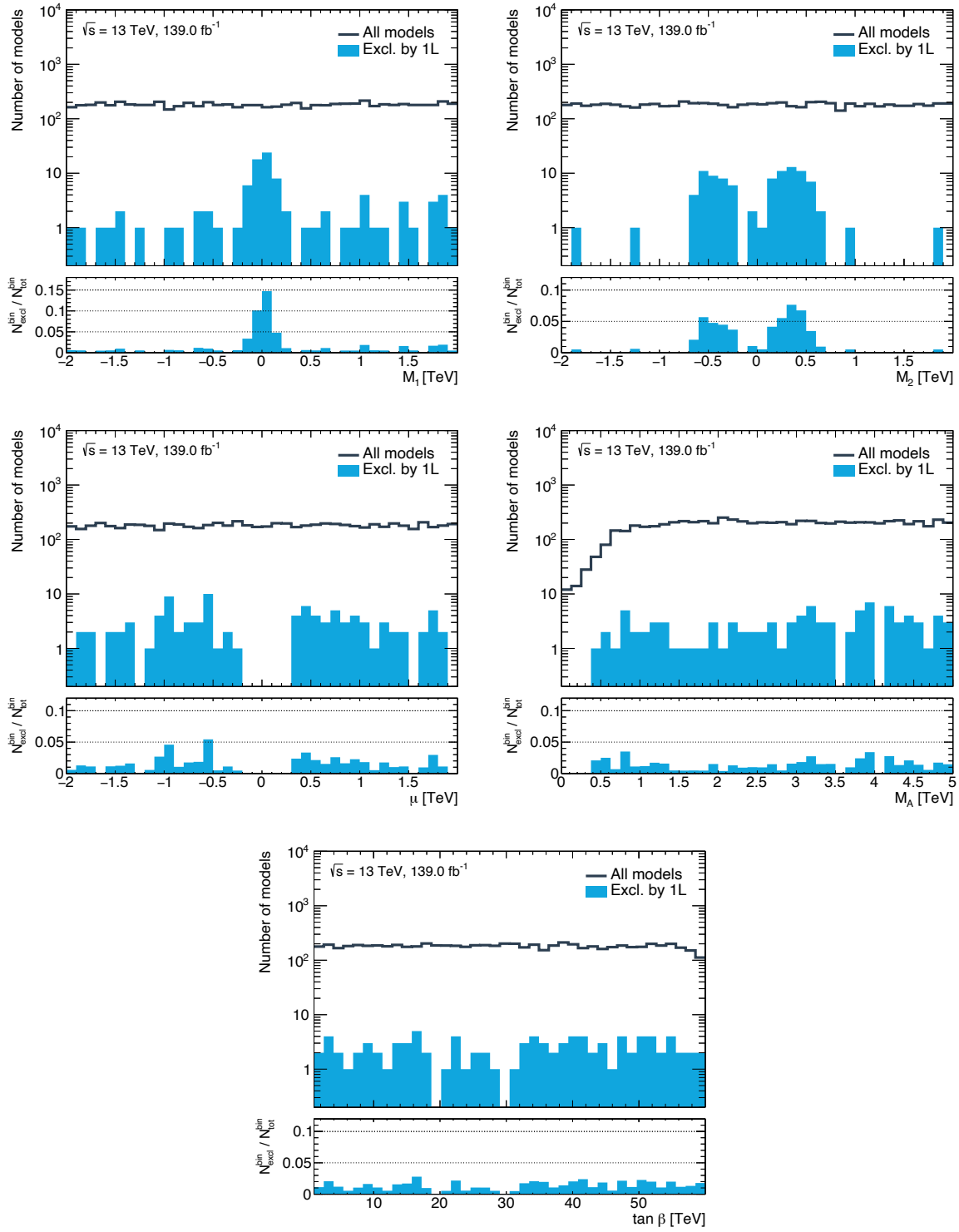

Figure 11.6: Bin-by-bin number of excluded models as a one-dimensional function of the pMSSM parameters sampled relevant to the electroweak sector. The bin-wise fraction of excluded models, $N^{\text{bin}}_{\text{excl}}/N^{\text{bin}}_{\text{total}}$, is shown in the lower pad. All models are evaluated using the simplified likelihood of the 1ℓ search.

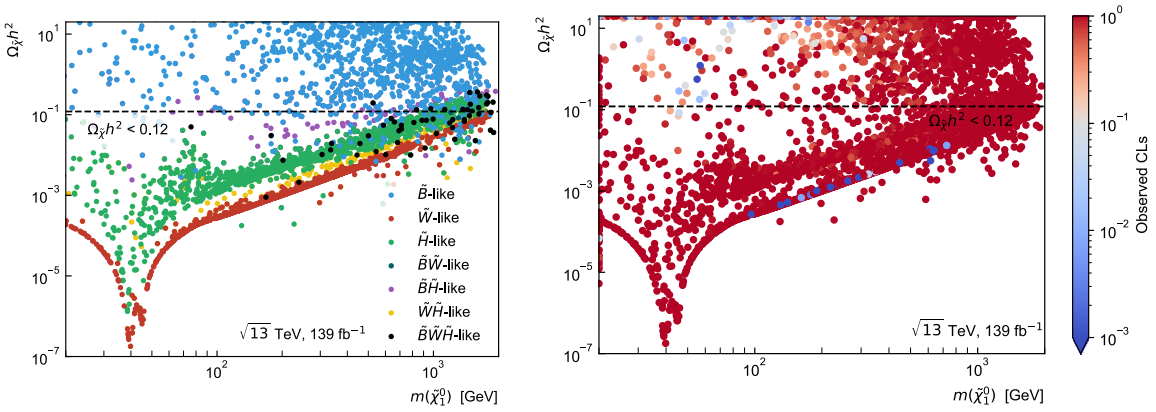

(a) **(b)**

Figure 11.7: Density of the pMSSM model points sampled in the plane spanned by the relic density and the $\tilde{\chi}_1^0$ mass. The model points are additionally shown as a function of (a) the nature of their $\tilde{\chi}_1^0$ and (b) the observed CL_s value obtained for 139 fb^{-1} of data using the 1ℓ search. The horizontal dashed line represents the DM relic density measurement by the Planck collaboration, interpreted as an upper limit $\Omega_{\tilde{\chi}}h^2 < 0.12$ such that the $\tilde{\chi}_1^0$ can be a sub-dominant DM component.

direct constraints on the trilinear scalar couplings (A_t, A_b, A_τ), and the remaining gluino and third generation squark mass parameters (M_3, $m_{\tilde{Q}_3}$, $m_{\tilde{u}_3}$, $m_{\tilde{d}_3}$) is observed. As can be seen from fig. C.9, the 1ℓ search excludes values of these parameters across the entire range originally sampled.

11.4.3 Impact on dark matter relic density

The $\tilde{\chi}_1^0$ cosmological abundance in dependence of its type and mass is shown in fig. 11.7(a). The measurement of the DM relic density by the Planck mission is shown as dashed line and interpreted as upper limit on the DM relic density, allowing the $\tilde{\chi}_1^0$ to be a sub-dominant DM component.

Some interesting features can be highlighted. First, most of the models sampled with bino-like $\tilde{\chi}_1^0$ result in a cosmological abundance $\Omega_{\tilde{\chi}}h^2$ incompatible with the result from Planck. Of the pMSSM models sampled in this work, only models containing a $\tilde{\chi}_1^0$ with a considerable wino or higgsino component satisfy $\Omega_{\tilde{\chi}}h^2 < 0.12$ over a large range of $m(\tilde{\chi}_1^0)$. Models with $m(\tilde{\chi}_1^0) \simeq m(Z)/2$ produce especially low values in $\Omega_{\tilde{\chi}}h^2$ as the $\tilde{\chi}_1^0$ can resonantly annihilate through s-channel Z exchange. This is the so-called *Z-funnel* [288]. A similar funnel exists around $m(h)/2$ but is not visible in fig. 11.7(a) due to an additional resonant process: co-annihilation of a nearly mass-degenerate $\tilde{\chi}_1^\pm\tilde{\chi}_1^0$ pair at $m(W)/2$ through s-channel W exchange.

In practice, experimental constraints like e.g. the LEP limit of $m(\tilde{\chi}_1^\pm) \gtrsim 100\,\mathrm{GeV}$ (the actual limit depends on the exact configuration of the SUSY mass spectrum probed) rule out models with $|M_2|, |\mu| \lesssim 100\,\mathrm{GeV}$. The effect of this in the $\Omega_{\tilde{\chi}}h^2$–$m(\tilde{\chi}_1^0)$ plane is shown in fig. C.10, revealing that models containing a $\tilde{\chi}_1^0$ with a large wino or higgsino component and $m(\tilde{\chi}_1^0) \lesssim 100\,\mathrm{GeV}$ are largely ruled out, leaving models with a bino-like $\tilde{\chi}_1^0$ as the only remaining possibility in this region. Although theoretically models with a bino-like $\tilde{\chi}_1^0$ could produce low $\tilde{\chi}_1^0$ relic density

values through the Z- and h-funnels, in practice such models are not sampled in this thesis due to the sampling technique used. Oversampling this region should however still reveal the typical Z- and h-funnels for models with a bino-like LSP [76, 75]. If the $\tilde{\chi}_1^\pm/\tilde{\chi}_2^0$ masses of such models fall into the range where the 1ℓ search is sensitive,i.e. $\tilde{\chi}_1^\pm\tilde{\chi}_2^0$ pair-production has high enough cross section, the 1ℓ search can be excepted to exclude a sizeable fraction of these models, thus warranting additional, dedicated scans using experimental constraints in the sampling priors.

Although of limited use due to the limited number of models in the relevant parameter space, the impact of the 1ℓ search on the DM relic density can still be investigated with the models available. Figure 11.7(b) shows the $\tilde{\chi}_1^0$ cosmological abundance in dependence of its mass. Instead of encoding the nature of the $\tilde{\chi}_1^0$, the colour now encodes the observed CL_s value obtained by the 1ℓ search. By comparing with fig. 11.7(a) it can be seen that the majority of the models with a bino-like $\tilde{\chi}_1^0$ excluded by the 1ℓ search have a cosmological abundance not satisfying $\Omega_{\tilde{\chi}}h^2 < 0.12$. Through its limited sensitivity to some of the models with a wino-like $\tilde{\chi}_1^0$, the 1ℓ search is however still able to exclude some models with a compatible LSP relic density.

11.5 Discussion

Large-scale reinterpretations in high-dimensional SUSY model spaces are crucial in order to assess the sensitivity of SUSY searches in the context of realistic SUSY scenarios. The evaluation of signal models at smeared truth level in combination with the simplified likelihoods introduced in chapter 10 offers a computationally efficient but still reliable approach for such reinterpretations.

A reinterpretation of the 1ℓ search in a limited number of models sampled from the pMSSM with a focus on the electroweak sector revealed that the search is sensitive to SUSY scenarios beyond the canonical simplified model originally considered. In general, the simplified model phenomenology maps reasonably well onto a portion of the pMSSM parameter space. The sensitivity of the 1ℓ search towards pMSSM models is however negatively impacted by the competing decays $\tilde{\chi}_2^0 \to Z\tilde{\chi}_1^0$ and $\tilde{\chi}_2^0 \to h\tilde{\chi}_1^0$, a circumstance that breaks one of the main assumptions of the simplified model. In order to maximise the sensitivity of future searches to $\tilde{\chi}_1^\pm\tilde{\chi}_2^0$ pair-production in more complete SUSY scenarios, it is therefore crucial to target both decay modes at the same time. In searches targeting final states with one lepton, multiple jets and missing transverse momentum, both the b-jet multiplicity as well as the invariant mass of the jets originating from the decays $h \to b\bar{b}$ and $Z \to q\bar{q}$ can easily be used to construct disjoint[†] signal regions targeting both decay modes.

Beyond the combination of single decay modes, it could be worth targeting not only $\tilde{\chi}_1^\pm\tilde{\chi}_2^0$ production, but also $\tilde{\chi}_1^\pm\tilde{\chi}_1^\pm$ production at the same time in a single likelihood function. In ATLAS, work is ongoing to perform e.g. a 1ℓ search with dedicated signal regions targeting both $\tilde{\chi}_1^\pm\tilde{\chi}_2^0 \to WZ\tilde{\chi}_1^0\tilde{\chi}_1^0 \to \ell\nu_\ell q\bar{q}\tilde{\chi}_1^0\tilde{\chi}_1^0$ and $\tilde{\chi}_1^\pm\tilde{\chi}_1^\pm \to WW\tilde{\chi}_1^0\tilde{\chi}_1^0 \to \ell\nu_\ell q\bar{q}'\tilde{\chi}_1^0\tilde{\chi}_1^0$ at the same time.

Finally, the impact of the 1ℓ search on the DM relic density was discussed. Due to the parameter ranges chosen during sampling and the lack of experimental constraints applied, many models

[†] Building signal regions that are not orthogonal to each other prevents the construction of a single likelihood and thus does not allow statistical combination.

sampled are not directly relevant to the DM phenomenology. Only a small number of models with a bino-like $\tilde{\chi}_1^0$ are sampled in the Z- and h-funnel region where $\Omega_{\tilde{\chi}} h^2 < 0.12$ is satisfied. Outside of these two funnels, models with a bino-like $\tilde{\chi}_1^0$ only satisfy the relic density constraint for $\tilde{\chi}_1^\pm$ and $\tilde{\chi}_1^0$ masses outside of the parameter space that the 1ℓ search is sensitive to. In order to be able to further investigate the impact of the 1ℓ search on DM observables—especially in the Z and h-funnels—a different sampling technique would need to be adopted and models with bino-like $\tilde{\chi}_1^0$ need to be oversampled in the relevant region of the parameter space.